PERGAMON

Applied Thermal Engineering 20 (2000) 1297–1314

APPLIED THERMAL ENGINEERING

www.elsevier.com/locate/apthermeng

Heat transfer analysis of low thermal conductivity solar energy absorbers

P.T. Tsilingiris

Department of Energy Engineering, Technological Educational Institution (TEI) of Athens, A. Spiridonos street, GR 122 10, Egaleo, Athens, Greece

Received 3 August 1999; accepted 25 October 1999

Abstract

Polymers have been proven to be high potential low-cost materials for the design and mass production not only for ordinary solar water heaters but also for very simple large size, modular solar collectors, suitable for easy erection of large solar heating plants. Their major drawback for solar–thermal conversion applications is their low thermal conductivity, which prohibits their use unless an appropriate absorber design is employed. The low thermal conductivity of polymers has imposed the need of a particular absorber design, which is basically composed of a pair of dark, closely spaced parallel plates at the top of which solar radiation is absorbed, forming a thin channel for the flow of the heat transfer fluid. The aim of the present work is to investigate the particular limitations of this polymer plate absorber design, for a wide range of collector loss and convective heat transfer coefficients between heat transfer fluid and absorber plate. The aim is also to calculate the particular collector efficiency factors and conditions under which the associated collector performance parameters should be modified to account for the finite absorber plate conductance. This conductance was proven to be another decisive absorber design parameter, improper selection of which may probably lead to strong deterioration of the collector efficiency.

Keywords: Solar polymer absorber; Collector efficiency factor; Collector loss coefficient

1. Introduction

After a long time under the protective environment of government support policies, now it appears that the future of solar–thermal conversion technology will rely entirely on its economic viability and competitiveness in the free energy market. Owing to the relatively low current cost of conventional energy, solar equipment should be designed and

1359-4311/00/$ - see front matter
PII: S1359-4311(99)00091-5

Nomenclature

A	cross sectional area (m^2)
b	plate thickness (m)
D	diameter (m)
C	numerical constant (–)
F'	collector efficiency factor (–)
G	incident solar radiation (W m^{-2})
h	convective heat transfer coefficient (W m^{-2} K)
k	thermal conductivity (W m^{-1} K^{-1})
m	numerical constant (–)
n	numerical constant (–)
P	perimeter (m)
q	unit area energy rate (W m^{-2})
S	solar energy absorption (W m^{-2})
T	temperature (°C)
U	loss coefficient (W m^{-2} K^{-1})
W	absorber width (m)
$(\tau\alpha)$	transmittance–absorptance product (–)
δ	spacing between plates (m)

Subscripts

a	ambient
b	back, back plate
bf	back plate-fluid interface
c	copper
f	fluid
f1	top plate-fluid
f2	back plate-fluid
h	hydraulic
L	loss
n	normal
o	useful gain
p	top plate
pf	top plate-fluid interface
t	top

manufactured to perform reliably over a long time with minimum maintenance. Towards this aim, the provision of standardization and a quality approval procedure would be absolutely necessary for solar products that should last as long as the conventional mechanical installations in buildings.

However, the high cost of such components is dominated by the cost of advanced design and materials employed, as well as advanced manufacturing processes, which usually leads to a

considerably long pay-back time. An economically equivalent approach would be based on the development of simple, low-cost, innovative solar system design employing widely available recyclable materials, which although of a shorter life cycle, give a much early payback. This approach sometimes appears to be highly attractive especially for large solar heating plants, which represent capital intensive investments. Excellent market promotion prospects for large solar heating plants are expected especially when the package consisting of design, erection, maintenance and financing of the proposed low-cost systems is carried out by a specialised solar engineering company, which under a legal contract supplies measured energy to energy users at a beneficial cost for a period during which system costs and company profits will be recovered [19].

It has long been established that significant cost reduction of solar collectors cannot be made unless new design involving new materials and mass production are available. Innovative designs of all-polymer collectors have been proposed, tested and demonstrated long ago [4,5,7,11]. Although the potential of polymers is based on the possibility of developing large plastic solar collectors at a substantially low cost using mass production processes, their major limiting factor is the environmental tolerance. This usually leads to an accelerated degradation due to the exposure of collector parts to UV radiation, and their low thermal conductivity which may become a limiting factor unless an appropriate absorber design is implemented. The use of glass as a glazing material not only completely eliminates IR radiation losses directly from absorber, but also offers adequate UV protection for the polymer absorber and collector enclosure underneath.

According to the theory, the useful heat gain of a solar collector can simply be expressed as a function of the mean absorber plate temperature. To refer to a localized fluid temperature, the collector efficiency factor F' is defined in the familiar Hottel–Willier–Bliss model. Derivation of this factor is based on the assumption of a negligible temperature drop at a direction perpendicular to the plane of absorber plate, something which may not be always valid for low thermal conductivity polymer absorbers.

The purpose of this work is to present an analysis for the calculation of the collector efficiency factor for the widely known top absorbing plate polymer absorber design, which determines the collector performance parameters. The aim is also to investigate the particular design limitations of the specific absorber, as well as the conditions under which the associated collector performance parameters in the familiar Hottel–Willier–Bliss (HWB) model should be modified to account the effect of low thermal conductivity materials in the absorber design.

2. Material considerations

From the early steps of evolution of both solar and polymer science and technology, an appreciable amount of attention of solar system designers was concentrated on polymers, owing to their favorable properties for solar design. They are widely available low-cost materials, which lend themselves to a volume production of lightweight low-cost collectors tolerant to corrosion and freezing temperatures; however, their reliability, durability and long-term performance have not been fully demonstrated yet for solar heating plants. Polymer glazings are subject to degradation under the combined effect of elevated temperatures and

exposure to UV radiation unless UV absorption additives in the outer cover or special inhibitors are used. Although these additives will certainly appreciably expand the life cycle of collectors, they will also contribute to a proportional increase in cost.

Many surveys and reports have been carried out on polymers as solar collector materials [1,22] and significant developments were accomplished in the science and technology of special polymers for building construction and retrofit, as well as for glazing, during the last few decades. Thin-walled cellular polycarbonate materials in the form of transparent capillary structures or square honeycombs are being extensively employed as collector glazing materials [18] and were successfully demonstrated in the design and retrofit of energy efficient buildings [3]. Advanced microencapsulated liquid crystal epoxy and polycarbonate polymer films were investigated and are being developed as potential transmission switching glazing materials, suitable for the design of building construction elements [23]. Among the most suitable polymer materials for absorber design are those of the polyolefin group, like polyethylene and polypropylene and of the ethylene–propylene–diene-monomer (EPDM) group, known as synthetic rubbers. Among them, polyolefins are mainly suitable for the manufacturing of thermally extruded flat rigid absorbers, while EPDM materials are suitable for the production of flexible tubes or tube strips interconnected by flexible webs, mainly suitable as low temperature swimming pool heating collectors.

A literature review on the thermophysical properties of polymer materials indicates a relatively low thermal conductivity of acrylics and derivatives, ranging between 0.17 and 0.23 W m^{-1} K^{-1} [10,15,16,18,21]. The corresponding values of high density (HD) and ultra high density (UHD) polyolefins and EPDM which may be suitable low-cost, widely available collector–absorber materials for low and medium temperature applications, are around 0.35 and 0.15 W m^{-1} K^{-1}, respectively [6,10,15,16,21]. From this comparative review it becomes clear that the thermal conductivity of polymers is substantially (almost three orders of magnitude) lower than that of ordinary metallic absorber materials, something which is very crucial for their use in solar energy applications and makes the redesign of conventional tube and fin metal absorber absolutely necessary.

3. Collector and absorber design considerations

It has recently been proposed [20] that a reasonable cost, efficiency and durability compromise could possibly be obtained by using glass instead of polymers as a glazing material in low cost polymer absorbers. The basic collector design is shown in Fig. 1(a) in which, a polymer absorber (2) is enclosed in a thermal insulation collector container (3), sealed at the top with a single glass pane glazing (1). Glass, apart from its weight and fragility, has been proven to be an environmentally stable low-cost material, which may substantially improve the UV protection of polymer collector components underneath against degradation, because of its spectral filtering characteristics. Both polymer absorber and collector container are factory made modular parts, which are in-situ assembled for easy erection of large collector plants at a minimal cost and minimum plumbing. The absorbers are fitted on hard polymer thermal insulation container of appropriate dimensions, connected through polymer tubing and sealed at the top with glass panes supported at the edges of the container.

In the contemporary design of polymer absorbers, the efforts are concentrated on increasing the absorber surface in direct contact with the heat transfer fluid, something which is known as the fully wetted absorber design. A very good report on the design of polymer absorbers was carried out by Madsen and Goss [14]. Various simple polymer absorber designs have appeared in the literature among which worth noting is the EPDM parallel tube design shown in Fig. 1(b), which was extensively employed as low temperature swimming pool heating collectors or the polymer film water bag absorber, shown in Fig. 1(c) in glazed or unglazed collectors.

Current design trends are oriented towards the production of extruded polymer absorbers with small, closely spaced flow passages, offering extended wetted surfaces for optimal heat transfer. This absorber design is considered very promising for the production of large low-cost solar collectors, which is typically composed of a pair of dark parallel polymer plates with a heat transfer fluid stream flowing in between (see Fig. 1(d)). In this design, the incident solar

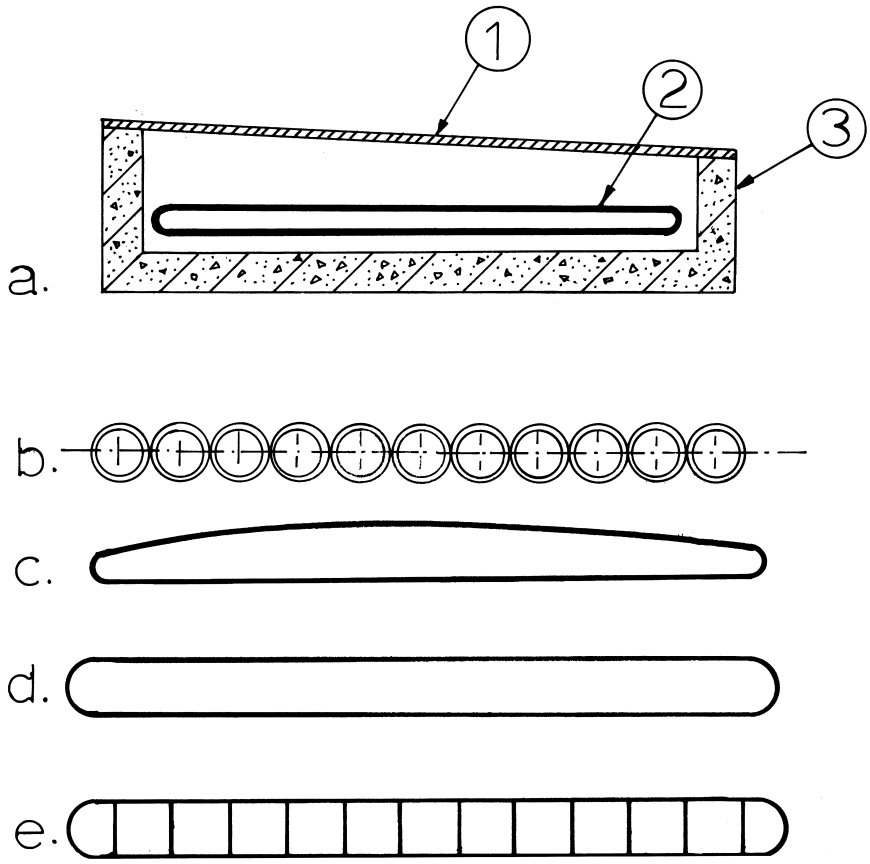

Fig. 1. The basic design of: a low-cost collector with a single glass pane glazing (1), a polymer absorber (2) and a thermal insullation enclosure (3) is shown in (1a). Various typical polymer absorber designs like EPDM tubing are shown in (1b), polymer film water bag in (1c), rigid parallel plate with or without support ribs is shown in (d) and (e), respectively (not to scale).

radiation is absorbed at the top plate and heat is transferred by conduction through the plate thickness and by convection to the heat transfer fluid flowing underneath.

An interesting alternative polymer absorber design comprises of two parallel plates made of extruded polymer, the top of which is transparent to solar radiation. In this design, the radiation absorption process is vastly different, since the incident solar radiation after passing through the top polymer–air interface is partly absorbed at the flowing water stream in the passage between polymer plates, before being completely absorbed at the back dark polymer plate. Since the full investigation of the theoretical analysis and processes of the corresponding design is beyond the scope of the present work, this may be the objective of future investigation.

4. Theoretical model and analysis

The subsequent analysis is presented for a polymer absorber design with a dark top absorbing plate, (Fig. 2). The conduction heat flow at the direction perpendicular to the absorber plane is assumed to be one-dimensional, for its negligible thicknesses as compared to the lateral plate dimensions. Also, two-dimensional effects in the large collector modules are assumed to be negligible because of the adequate thermal insulation at their periphery.

The spectral extinction coefficient of glass, especially of the low iron content quality, is almost uniform at the visible and near-IR band of the solar spectrum [8]. The incident solar radiation is partially absorbed while passing through the glass top glazing system before being absorbed at the top dark plate of the polymer absorber. The absorbed heat is partly dissipated to the environment by convection and radiation through the top glazing system. Heat is also

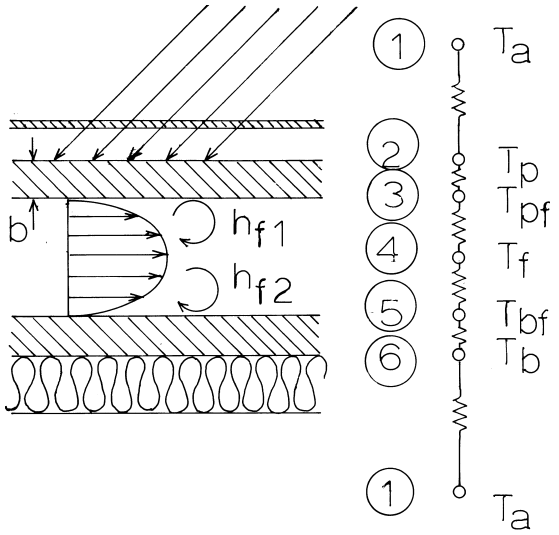

Fig. 2. The cross section of the top absorbing plate absorber (not in scale) with a plate thickness b and convective heat transfer coefficients h_{f1} and h_{f2}, corresponding to top and back plate, respectively, in a conventional flat plate solar collector, along with the corresponding nodes of the thermal network.

transferred by conduction through the polymer plate thickness and by convection to the heat transfer fluid flowing underneath. Convection and conduction heat transfer is also responsible for subsequent heat losses from the heated fluid to the environment through the back thermal insulation of the absorber.

The convective heat transfer coefficient between top or bottom polymer plates and heat transfer fluid may considerably vary, mainly depending on the particular absorber design or operating conditions and mass flow rates. This is due to the fact that for a particular hydraulic diameter of flow passage (defined as $D = 4\,A/P$, where A and P are the cross section area and the wetted perimeter, respectively), and the particular mass flow rate the Reynolds number may vary in a considerably wide range. The hydraulic diameter for a rectangular flow passage of a width W is calculated as

$$D = \frac{2\delta}{(1 + \delta/W)} \tag{1}$$

where δ is the polymer plate spacing. When $(\delta/W) \rightarrow 0$, as usually happens in practice, the hydraulic diameter becomes twice the δ. Using this quantity as a characteristic length in the definition of Reynolds number, the familiar correlations for internal flows in circular cross-sections can be applied at least to a first approximation for rectangular passages, according to the fundamental theory [12]. Assuming that transition flow occurs at $Re > 2300$, and taking into consideration the usual mass flow rates per collector unit area in conventional and even in low flow collectors (of about less than 0.02 and 0.002 kg m^{-2} s^{-1}, respectively), and a typical design of water heating flat plate collector, it would be reasonable to expect for a fully developed flow at a small Reynolds number, typically around 80, something which practically suggests that the flow almost always is laminar flow. Although for laminar flow the results appear to be less accurate than for turbulent flow, the theory predicts a very small Nusselt number for fully developed flow, irrespective of flow velocity, corresponding to a convective heat transfer coefficient for a circular cross-section typically around 150 W m^{-2} K^{-1}, something which is also confirmed by the classical literature [9]. For shorter than the entry lengths, which according to the theory occurs at Graetz numbers around 20,

$$Gr = \frac{Re_D \cdot Pr}{(x/D)} \simeq 20 \tag{2}$$

the corresponding local Nusselt number increases significantly as approaching the flow entry, which suggests a corresponding increase of the local convective heat transfer coefficient h_f. For the thermophysical properties of water and water–ethylene glycol solutions with a flow passage of 10 mm at typical operating conditions, the theory predicts an entry length in the order of 0.4 m, which although is negligible as compared to the length of large modular collector arrays, it may become a significant fraction of smaller collector units of typically 2 m length.

For turbulent flow that cannot be always exempted especially for operation with higher mass flow rates or special absorber designs with very narrow flow passages, the theory predicts appreciably higher Nusselt numbers, which are given by the familiar correlation,

$$Nu_D = C \cdot Re_D^m \cdot Pr^n \tag{3}$$

where C, m and n are numerical constants equal to 0.023, 0.80 and 0.333, respectively. Although turbulent flow would be rather unusual to occur in practical designs and operating conditions, the estimated heat transfer coefficient may substantially vary, mainly depending on mass flow rates and the characteristic length corresponding to the polymer plate distance.

However, it should be mentioned that, in noncircular cross-sections with sharp corners and large aspect ratios, the local convective heat transfer coefficient may appreciably vary around the periphery approaching very small values at the corners. For such conditions, the Nusselt number corresponding to fully developed laminar flow in circular cross-sections should be appropriately corrected to account for the flow in rectangular cross-sections [13]. The corrected Nusselt number is proportional to the aspect ratio of the rectangular cross-section, which, for $(\delta/W)\rightarrow 0$ may become twice as high as its predicted value for the circular cross-section. This leads to an appreciably higher convective heat transfer coefficient, which is proportional to the aspect ratio of the rectangular cross-section, and may become twice as high as its predicted value for a circular cross-section. Therefore, in order to correlate results corresponding to a wide range of design and operational conditions, a convective heat transfer coefficient between 75–300 and 300–800 W m^{-2} K^{-1} were considered. Although the highest values of the second group are rather unusual to occur in practice, their consideration is rather instructive for the investigation of the fundamental behavior and the limiting trends of the crucial collector parameters.

The heat transfer fluid is assumed to be completely opaque to IR radiation so that radiative heat exchange between top and back absorber plates can be completely ignored. The effect of ribbing conductance can also be completely ignored owing to the low thermal conductivity of absorber materials.

For the top absorbing plate absorber with h_{f1} and h_{f2} (the top and convective heat transfer coefficients shown in Fig. 2, where the nodes of the thermal network are also shown), the steady-state heat balance expressions at the nodes 2–6 are,

$$S_t - U_t \cdot (T_p - T_a) - \frac{k_p}{b} \cdot (T_p - T_{pf}) = 0 \tag{4}$$

$$\frac{k_p}{b} \cdot (T_p - T_{pf}) - h_f 1 \cdot (T_{pf} - T_f) = 0 \tag{5}$$

$$h_{f1} \cdot (T_{pf} - T_f) - q_o - h_{f2}.(T_f - T_{bf}) = 0 \tag{6}$$

$$h_{f2} \cdot (T_f - T_{bf}) - \frac{k_p}{b}.(T_{bf} - T_b) = 0 \tag{7}$$

$$\frac{k_p}{b} \cdot (T_{bf} - T_b) - U_b \cdot (T_b - T_a) = 0 \tag{8}$$

with S_t the absorbed solar radiation at the top absorber surface as calculated in the literature [9]. For the derivation of the top absorbing plate parameters, it would be necessary to eliminate the variables T_p, T_{pf}, T_{bf} and T_b in the expressions (4)–(8). Therefore, eliminating T_p

from the expressions (4) and (5) yields,

$$T_{pf} = \frac{(S_t + U_t \cdot T_a)/(U_t + k_p/b) + h_{f1} \cdot T_f/(k_p/b)}{U_t/(k_p/b + U_t) + h_{f1}/(k_p/b)} \tag{9}$$

In a similar way, eliminating T_b from Eqs. (7) and (8) yields, respectively,

$$T_{bf} = \frac{(U_b/\{U_b + k_p/b\}) \cdot T_a + (h_{f2}/\{k_p/b\})T_f}{(U_b/\{U_b + \{k_b/b\}\}) + (h_{f2}/\{k_b/b\})} \tag{10}$$

Substituting T_{pf} and T_{bf} from expressions (9) and (10), respectively, into the expression (6) and rearranging, yields

$$\begin{aligned} q_o = {} & \frac{h_{f1} \cdot S_t}{U_t + h_{f1} + h_{f1} \cdot U_t/(k_p/b)} + \left(\frac{h_{f1}^2}{h_{f1} + \{U_t \cdot (k_p/b)/(U_t + (k_p/b))\}} \right. \\ & \left. - \frac{h_{f2}^2}{h_{f2} + \{U_b \cdot (k_p/b)/(U_b + (k_p/b))\}} - h_{f1} - h_{f2} \right) \cdot T_f \\ & + \left(\frac{h_{f1} \cdot U_t}{U_t + h_{f1} + h_{f1} \cdot U_t/(k_p/b)} + \frac{h_{f2} \cdot U_b}{U_b + h_{f2} + h_{f2} \cdot U_b/(k_p/b)} \right) \cdot T_a \end{aligned} \tag{11}$$

After algebraic manipulations and rearrangements, the previous expression becomes,

$$\begin{aligned} q_o = {} & \frac{1}{1 + U_t/(k_p/b) + U_t/h_{f1}} \\ & \cdot S_t - \left[\frac{U_t}{1 + U_t/h_{f1} + U_t/(k_p/b)} + \frac{U_b}{1 + U_b/h_{f2} + U_b/(k_p/b)} \right] \cdot (T_f - T_a) \end{aligned} \tag{12}$$

Eq. (12) is an expression of the collector useful heat gain as a function of S_t and $\Delta T = T_f - T_a$. Aiming to derive an expression for the useful heat in a more convenient similar to Hottel–Willier–Bliss form, it would be necessary to rearrange the previous expression so as,

$$\begin{aligned} q_o = {} & \frac{1}{1 + U_t \cdot (\{1/(k_p/b)\} + (1/h_{f1}))} \\ & \cdot \left[S_t - \left(U_t + U_b \cdot \frac{h_{f2} \cdot [U_t + h_{f1} + h_{f1} \cdot U_t/(k_p/b)]}{h_{f1} \cdot [U_b + h_{f2} + h_{f2} \cdot U_b/(k_p/b)]} \right) \cdot (T_f - T_a) \right] \end{aligned} \tag{13}$$

which is the familiar Hottel–Willier–Bliss (HWB) equation,

$$q_o = F' \cdot [S_t - U_L \cdot (T_f - T_a)] \tag{14}$$

where,

$$F' = \frac{1}{1 + U_t.\left(\frac{1}{k_p/b} + \frac{1}{h_{f1}}\right)} \tag{15}$$

and

$$U_L = U_t + U_b \cdot (h_{f2}/h_{f1}) \cdot \frac{U_t \cdot (k_p/b) + h_{f1} \cdot (k_p/b) + h_{f1} \cdot U_t}{U_b \cdot (k_p/b) + h_{f2} \cdot (k_p/b) + h_{f2} \cdot U_b} \tag{16}$$

Expression (15) is the collector efficiency factor for the top absorbing parallel plates with finite thermal conductivity as reported, without derivation, by O'Brien-Bernini and McGowan [17]. For thin metal absorbers, the ratio (k_p/b) becomes infinite, and expression (15) becomes similar to the one derived by Bliss [2], for a collector with a parallel flow beneath a metal flat plate.

For $h_{f1} \gg h_{f2}$ or for $U_b \rightarrow 0$, which happens either when convective heat transfer coefficient at the back plate is appreciably lower than that at the top absorbing plate, or when the back loss conductance is negligible, the second term of the right-hand side of Eq. (16) becomes very small and is simplified to,

$$U_L = U_t \tag{17}$$

Although the top absorbing plate is at a higher temperature than the back plate, the associated convective heat transfer coefficients are usually expected to be close enough to justify the assumption of $h_{f1} = h_{f2} = h_f$. Then, Eq. (16) is simplified to,

$$U_L = U_t + U_b \cdot \frac{U_t + h_f + h_f \cdot U_t/(k_p/b)}{U_b + h_f + h_f \cdot U_b/(k_p/b)} \tag{18}$$

For appreciably large values of k_p/b as happens with metal absorbers, expression (18) becomes,

$$U_L = U_t + U_b \cdot \frac{U_t/h_f + 1}{U_b/h_f + 1} \tag{19}$$

Then, when $U_t \ll h_f$ and $U_b \ll h_f$, the expression (19) becomes

$$U_L = U_t + U_b \tag{20}$$

5. Results and discussion

The collector efficiency factor as calculated by the expression (15) for a top absorbing plate absorber is plotted in Figs. 3 and 4, as a function of k_p/b, with the top convective heat transfer coefficient h_f and collector top loss coefficient U_t, as parameters.

In Fig. 3, the collector efficiency factor is plotted for relatively low convective heat transfer coefficients of $h_f = 75$, 150 and 300 W m^{-2} K^{-1}, corresponding to each group of the three solid, broken and dotted lines, respectively, while the topmost and the following two lines of each group underneath correspond to a collector top loss coefficient of $U_t = 3$, 5 and 7 W m^{-2} K^{-1}, respectively.

In Fig. 4, the collector efficiency factor is plotted in a similar way as the function of the k_p/b ratio for a range of relatively high convective heat transfer coefficients of $h_{f1} = 800$, 500 and 300 W m^{-2} K^{-1}, corresponding to each group of the three solid, broken and dotted lines, respectively, with the topmost, and the following two lines underneath corresponding again to top loss coefficients of $U_t = 3$, 5 and 7 W m^{-2} K^{-1}, respectively.

It is seen that the group of lines in Fig. 3, when the k_p/b ratio ranges between 200 and 1000, is almost independent of k_p/b ratio depending solely on h_f and U_t, since an increase of h_f leads to a higher heat transfer rate of absorbed energy to the heat removing fluid. At k_p/b lower than 200, which corresponds a $b > 1.5$ mm, there is a dramatic decrease in collector efficiency factor owing to the corresponding decrease in the thermal conductance of the absorber plate. Specifically, values lower than 100 lead to an enormous decrease in collector efficiency factor, which makes the use of the absorber material possibly unacceptable.

For the range of higher heat transfer coefficients as shown in Fig. 4, and for values of k_p/b ratio ranging between 200 and 1000, the collector efficiency factor is only slightly dependent on

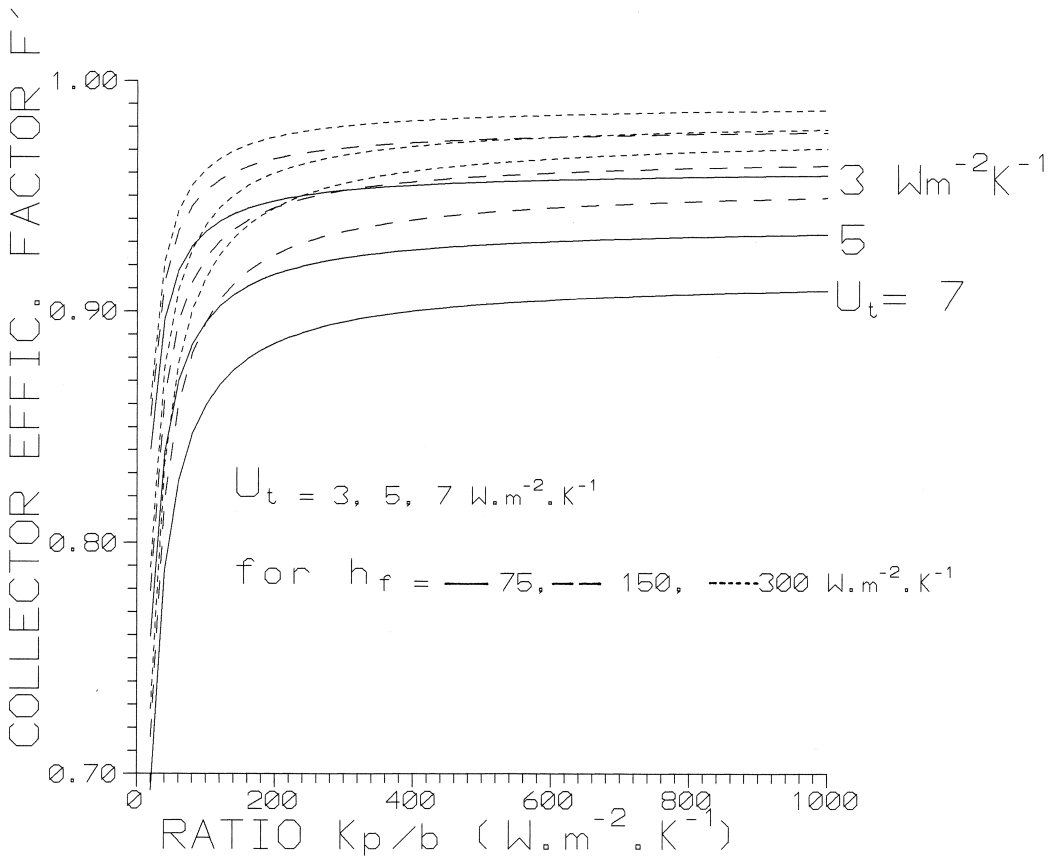

Fig. 3. The collector efficiency factor for a top absorbing plate design is plotted as a function of k_p/b. All solid, broken and dotted lines correspond to a group of lower convective heat transfer coefficients, $h_{f1} = h_{f2} = h_f = 75$, 150 and 300 W m^{-2} K^{-1}, respectively, with the top, and the lower two lines underneath correspond to $U_t = 3$, 5 and 7 W m^{-2} K^{-1}, respectively.

k_p/b, while it also exhibits a dramatic decrease at values lower than 200. From a comparative inspection between Figs. 3 and 4, it is derived that higher collector efficiency factors are expected for higher convective heat transfer coefficients, owing to the more efficient heat transfer to the flowing stream, which leaves the absorber plate at relatively low temperatures.

The first derivatives of F' as given from expression (15) in terms of the variables U_t and h_f are,

$$\left(\partial F'/\partial U_t\right) = -\frac{\left(\frac{1}{k_p/b} + \frac{1}{h_f}\right)}{\left[1 + U_t \cdot \left(\frac{1}{k_p/b} + \frac{1}{h_f}\right)\right]^2} \tag{21}$$

and

$$\left(\partial F'/\partial h_f\right) = \left(\frac{U_t}{h_f^2}\right)/\left[1 + U_t \cdot \left(\frac{1}{k_p/b} + \frac{1}{h_f}\right)\right]^2 \tag{22}$$

It will always be expected, in practice, that $h_f > U_t$. Therefore, the condition

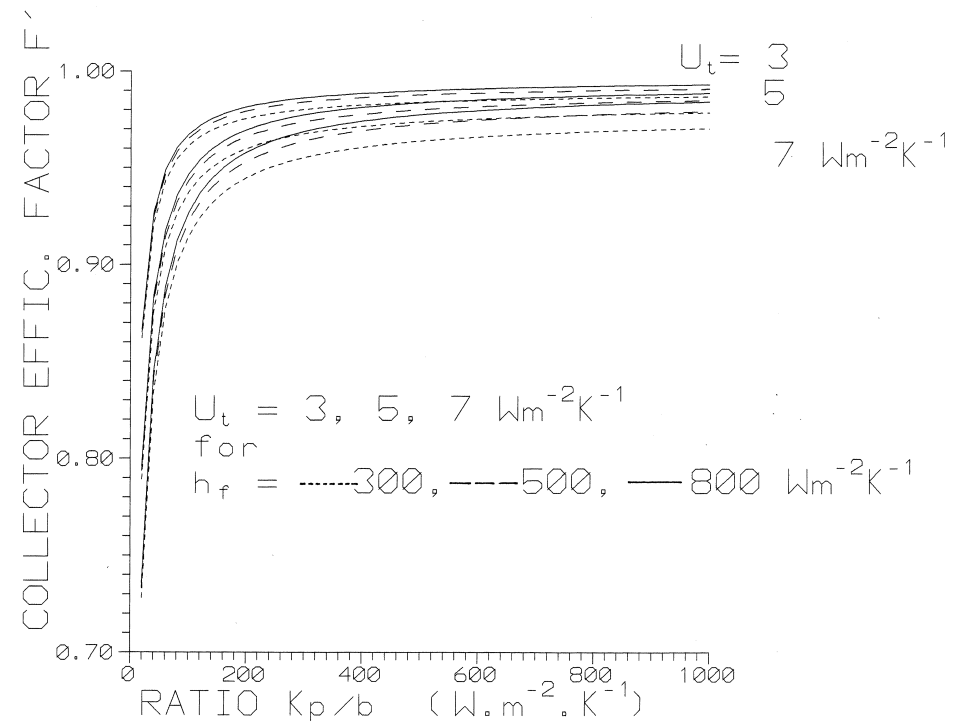

Fig. 4. The collector efficiency factor for the same absorber design and top loss coefficients as plotted in Fig. 3. The solid, broken and dotted lines in this plot correspond to a group of higher convective heat transfer coefficients $h_{f1} = h_{f2} = h_f = 300$, 500 and 800 W m^{-2} K^{-1}, respectively.

$$h_f^2 + \left(k_p/b\right) \cdot (h_f - U_t) > 0 \tag{23}$$

will always be satisfied. Division of the previous expression by the quantity $h_f^2 \cdot (k_p/b)$ and following algebraic manipulations yields,

$$\frac{1}{k_p/b} + \frac{1}{h_f} > \frac{U_t}{h_f^2} \tag{24}$$

which indicates that although the effect of the variables h_f and U_t on F' is of opposite sign, the effect of U_t is stronger than h_f, as can be clearly seen from the spacing between the corresponding equal h_f curves as compared to those of equal U_t.

In Figs. 5 and 6, the derived collector loss coefficient from the expression (16) is plotted against the k_p/b ratio, with the top loss and convective heat transfer coefficient as parameters, for a fixed back loss coefficient of $U_b = 2$ and 4 W m^{-2} K^{-1}, respectively. It is seen from these plots that the collector loss coefficient is slightly dependent on k_p/b for values ranging between 200 and 1000, being almost equal to the sum of top and back loss coefficients, something

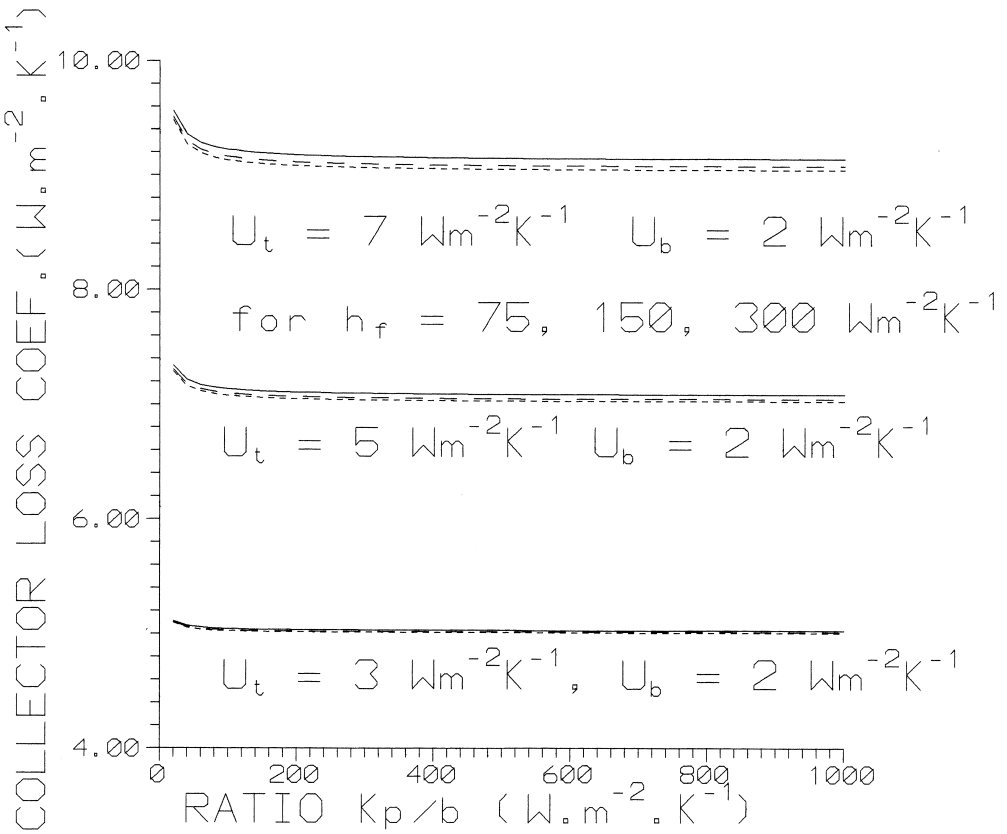

Fig. 5. The collector loss coefficient was plotted for a top absorbing plate absorber design as a function of k_p/b for $h_{f1} = h_{f2} = h_f = 75$, 150 and 300 W m^{-2} K^{-1} corresponding to solid, broken and dotted lines, respectively, for a top loss coefficient of $U_t = 3$, 5 and 7 W m^{-2} K^{-1} and for a fixed back loss coefficient of $U_b = 2$ W m^{-2} K^{-1}.

which is expected for negligible peripheral and edge collector losses. However, for values of k_p/b lower than 200, the collector loss coefficient should appropriately be modified to account for the increasing thermal resistance of the top absorber plate. At these small values of k_p/b, the heat transfer rate to the fluid stream is significantly reduced, something which leads to higher top absorber plate temperatures and significant corresponding increase of heat losses.

The effect of the convective heat transfer coefficient $h_{f1} = h_{f2} = h_f$ on the collector loss coefficient is small, irrespective of k_p/b ratio, as shown from both figures, with a trend of becoming stronger for higher top loss coefficients as shown by the increased spacing between each group of 75 (solid), 150 (broken) and 300 W m^{-2} K^{-1} (dotted) lines. A lower convective heat transfer coefficient h_f, generally leads to a higher collector loss coefficient owing to lower heat transfer rates leaving the absorber surface at a higher temperature.

Although the effect of different convective heat transfer coefficients between the top or back plates and heat transfer fluid has explicitly been taken into account in the preceding analysis, a uniform heat transfer coefficient was assumed throughout the absorber flow passage for the

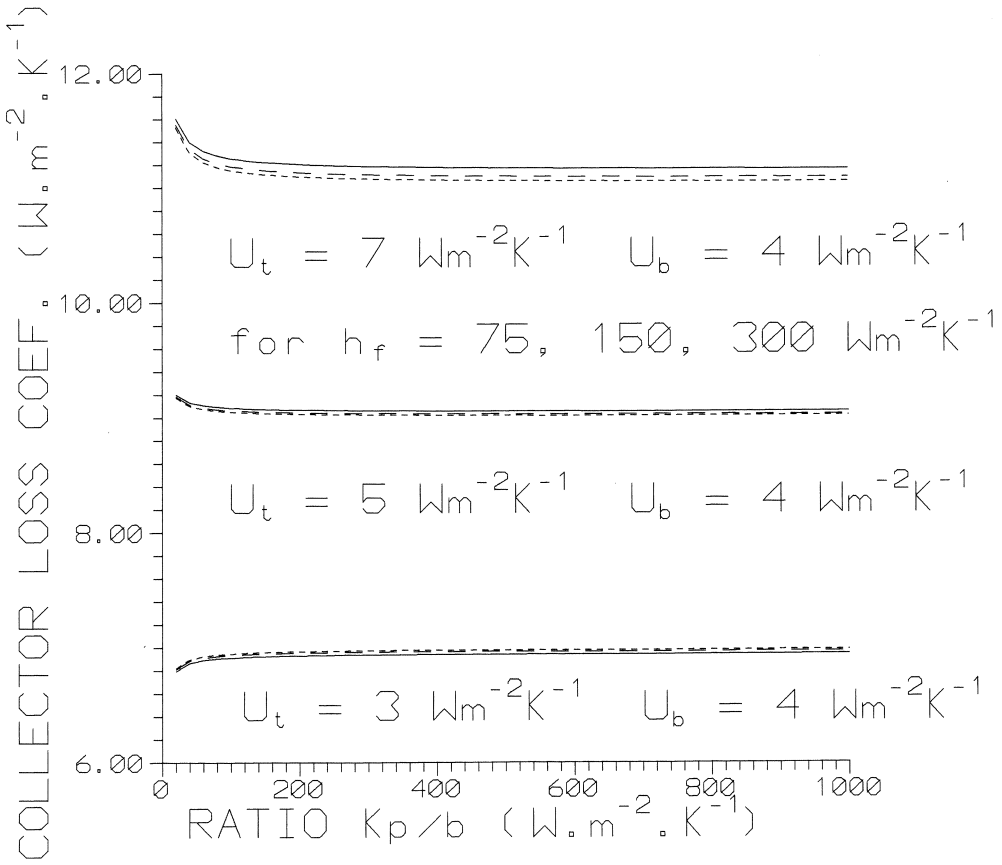

Fig. 6. The collector loss coefficient factor was plotted for a top absorbing plate absorber design as a function of k_p/b, for similar parameters as in Fig. 5 except of the back loss coefficient U_b, which is now fixed at $U_b = 4$ W m^{-2} K^{-1}.

presentation of results in Figs. 3–6. Although the top and back polymer plates are generally at different temperatures, a substantial difference between the associated heat transfer coefficients is not usually expected. However, to account for unusual situations involving a substantial temperature gradient between both plates or two phase flows, collector loss coefficient calculations were carried out for $h_{f1} = 150$ W m^{-2} K^{-1} and $h_{f2}/h_{f1} = 2$ and 0.5, and were compared to $h_{f2}/h_{f1} = 1$. The results can be seen in Fig. 7 in which the collector loss coefficient was plotted against the k_p/b ratio, with U_t as a parameter for a fixed $h_{f1} = 150$ W m^{-2} K^{-1} and $h_{f2} = 300$ W m^{-2} K^{-1} (broken line), 150 W m^{-2} K^{-1} (solid line) and 75 W m^{-2} K^{-1} (dotted line). It is confirmed that the effect of convective heat transfer coefficient imbalance is generally small for the range of investigated h_{f2}/h_{f1} ratios, and uniform over the entire range of k_p/b ratio. The broken and dotted lines correspond to a slightly higher or lower collector loss coefficient, respectively, owing to relatively low or high heat transfer rates which lead to a slightly higher or lower absorber temperature and collector loss coefficient, respectively.

According to the results of the preceding analysis it becomes clear that for certain values of the k_p/b parameter, the effect of polymer plate conductance may strongly influence the collector efficiency and loss coefficients. More specifically, values of the parameter k_p/b lower than 200, lead to a significant decrease of the collector efficiency factor and increase of the collector loss coefficient, something that may have a detrimental effect on the collector

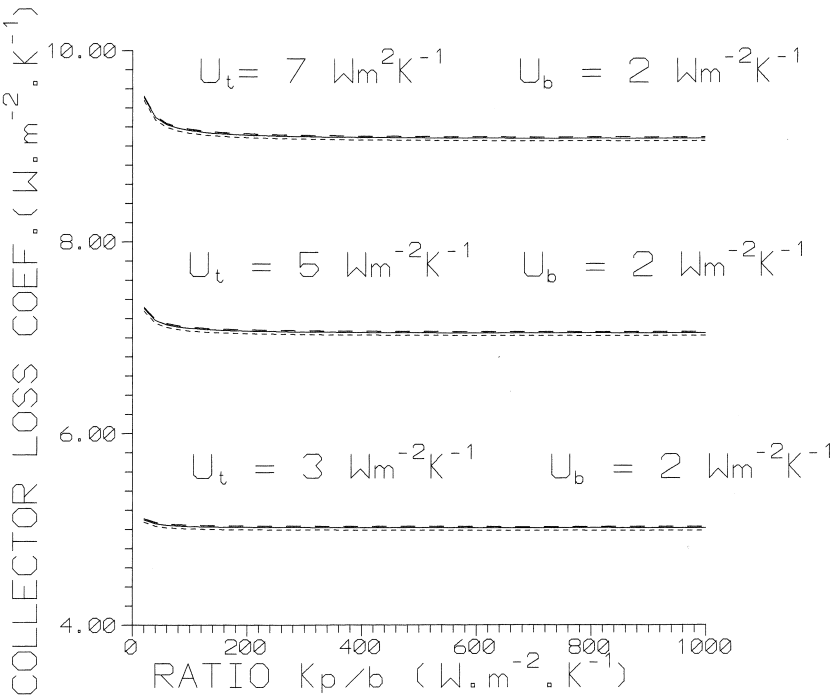

Fig. 7. The effect of convective heat transfer coefficient imbalance on collector loss coefficient for a top absorbing plate absorber design, which is plotted against k_p/b for a $U_t = 3$, 5 and 7 W m^{-2} K^{-1} and a fixed $U_b = 2$ W m^{-2} K^{-1} and $h_{f1} = 150$ W m^{-2} K^{-1}. Solid lines correspond to $h_{f2} = 150$ W m^{-2} K^{-1}, while broken and dotted lines to $h_{f2} = 300$ and 75 W m^{-2} K^{-1}, respectively.

efficiency. To investigate the effect of this parameter which appears to be an important design criterion for polymer absorbers on collector performance, a reference flat plate collector of an ordinary, single pane design was considered with a top absorbing polymer plate absorber, with a $k_p = 0.3$ W m^{-1} K^{-1} and a fixed $(\alpha\tau)_n = 0.85$ and $U_L = 8$ W m^{-2} K^{-1}. To simplify the comparison, the temperature distribution in the flow direction was completely ignored. Then, the Hottel–Willier–Bliss equation in terms of the average fluid temperature over the absorber surface becomes,

$$\eta = (\alpha\tau)_n F' - U_L \cdot F' . \left[(T_f - T_a)/G\right] \tag{25}$$

Four top absorber plate collector designs with progressively low absorber plate conductances of $(k_p/b) =$ 300, 100, 60 and 30 W m^{-2} K^{-1} were investigated, corresponding to plate thicknesses 1, 3, 5 and 10 mm. The plate conductance of 300 corresponds to a good absorber design, while conductances of 100 and 60 are considered to represent an average to poor absorber design. Finally, the conductance of 30 W m^{-2} K^{-1} corresponds to an unsuccessful absorber design.

For a fixed $h_f = 100$ W m^{-2} K^{-1} and the reference numerical parameters, the corrections imposed by the finite thermal conductance of the polymer plate to collector parameters through the expressions (14) and (15) lead to the pair of numerical values of $(\alpha\tau)_n \cdot F'$, $U_L \cdot F'$ equal to (0.787, 7.503), (0.758, 7.279), (0.732, 7.070) and (0.674, 6.602), corresponding to plates of 1, 3, 5 and 10 mm thickness. The results were comparatively plotted in Fig. 8, which represents the collector heat collection efficiency in terms of the $(T_f - T_a)/G$ parameter. The top broken and the following three lines underneath correspond to plate thicknesses of 1, 3, 5 and 10 mm. In the same plot, the performance of a tube and copper sheet absorber single-pane flat plate collector of a good design with identical $(\alpha\tau)_n$ and U_L parameters was comparatively plotted with a solid line. For a 1 mm copper sheet and a 10 mm diameter tube 6 cm apart, the theory [9] predicts $F' = 0.872$, which leads to $(\alpha\tau)_n \cdot F' = 0.741$ and $U_L \cdot F' = 6.976$ W K^{-1}.

An inspection of the performance lines in Fig. 8 for the polymer absorber–collectors indicates that the performance reduction corresponding to an increase in plate thickness from 1 to 10 mm is substantially higher at lower values of the $(T_f - T_a)/G$ ratio. This is attributed to the relative effect of plate conductance (k_p/b) at values lower than 200 on F' and U_L, which is substantially stronger on F' as shown in Fig. 3. Apparently, an improper absorber design as shown by the lowest broken line corresponding to $k_p/b = 30$ W m^{-2} K^{-1} leads to a significant collector performance loss. For typical operating conditions corresponding to a value of $(T_f - T_a)/G$ around 0.32, a decrease in plate conductance from 300 to 80 and from 300 to 30 W m^{-2} K^{-1} leads to a corresponding performance reduction of 5% to more than 15%, respectively.

Further comparisons show that the copper absorber–collector behaves equally well or marginally better than the one with polymer absorber, only at a very small region corresponding to very high values of the ordinate variable $(T_f - T_a)/G$. However, for the rest whole region of lower ordinate values of $(T_f - T_a)/G$, its performance is lower than a well designed or at least marginally comparable to an average to poor design polymer absorber–collector, something which becomes very important taking into consideration the substantially high cost of the copper absorber–collector.

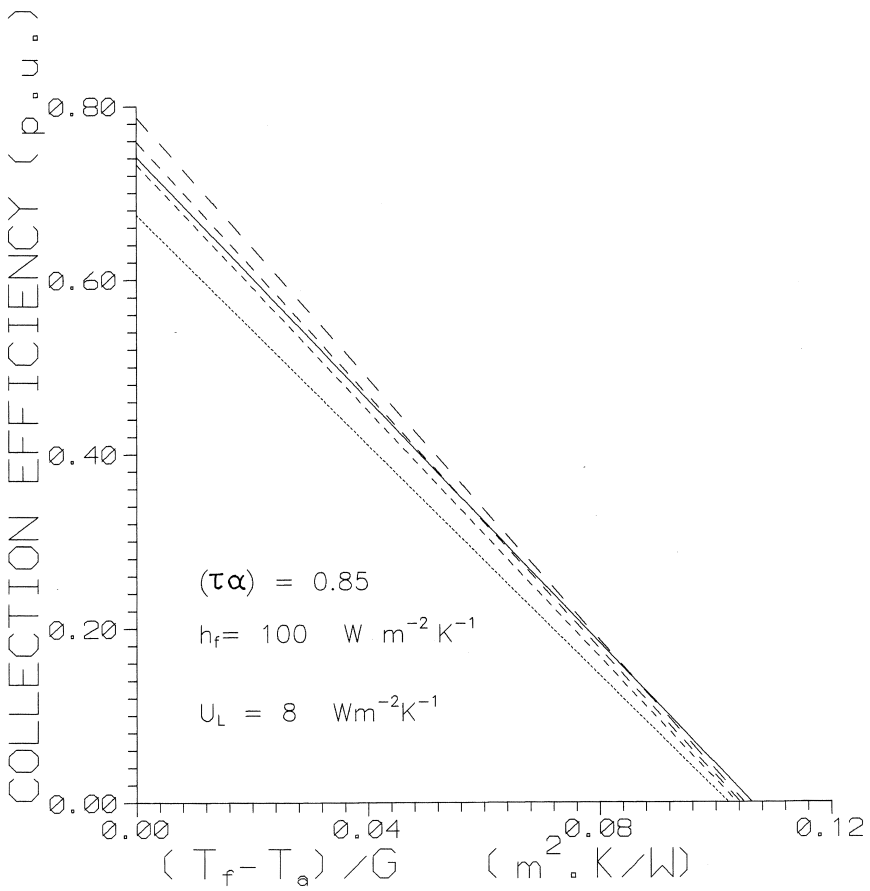

Fig. 8. Comparative performance lines for various collector–absorber designs. The top broken line and the following three broken lines underneath correspond to top absorbing polymer plates of thickness 1, 3, 5 and 10 mm, respectively. The solid line corresponds to a copper sheet and tube collector absorber with $k_c \cdot b = 0.35$ W K^{-1}.

6. Conclusions

An analysis was developed for the investigation of the conditions under which low thermal conductivity polymer materials could successfully be employed for the development and mass production of large, modular low-cost solar collectors that are vital for the promotion of large solar heating plants in the competitive environment of the free energy market. Towards this aim, a theoretical investigation was carried out for the calculation of collector efficiency factors for the parallel plate top absorbing polymer absorber design. The analysis allowed the determination of the collector performance parameters for a wide range of top or back collector loss and convective heat transfer coefficients and the investigation of conditions under which the collector performance parameters in the HWB equation should be modified to account for the effect of absorber plate conductance.

As seen from the analysis it appears that, the plate conductance (k_p/b), defined as thermal conductivity by the polymer plate thickness ratio, becomes a very important parameter in the

design of polymer absorber. According to the developed analysis it was found that when this parameter is lower than a certain critical value, the collector efficiency factor decreases dramatically, while the collector loss coefficient may significantly increase, leading to a substantial deterioration of collector performance. This critical value was estimated to be about 200, irrespective of the collector performance or operational parameters. For an average thermal conductivity of 0.33 and 0.14 W m^{-2} K^{-1} for polyolefins and EPDM, this typically corresponds to plate thicknesses of 1.6 and 0.7 mm, respectively.

References

[1] Best Don, New plastics head for higher temperatures, Solar Age, Feb. (1982) 51–52.
[2] R.W. Bliss, The derivation of several 'plate efficiency factors' useful in the design of flat-plate solar heat collectors, Solar Energy 3 (4) (1959) 55–64.
[3] P.O. Braun, A. Goetzberger, J. Schmid, W. Stahl, Transparent insulation of building facades — steps from research to commercial applications, Solar Energy 49 (5) (1992) 413–427.
[4] A.B. Casamajor, The application of shallow solat ponds for industrial process heat: case histories, in: Proc. A.S./ISES Silver Jubilee Congress, Atlanda, GA, 1979, pp. 1029–1032.
[5] A.F. Clark, W.C. Dickinson, Shallow solar ponds, in: W.C. Dickinson, P.N. Cheremisinoff (Eds.), Solar Energy Technology Handbook, Part A, Marcel Decker, New York, 1980, pp. 377–402.
[6] H. Gartman (Ed.), De Laval Engineering Handbook, McGraw Hill, New York, 1970.
[7] W.C. Dickinson, A.F. Clark, A. Iantuono, Shallow solar ponds for industrial process heat: the ERDA-SOHIO project, in: Proc. Joint AS/ISES and Solar Energy Soc Canada Conf., Winnipeg, Canada 5, 1975, pp. 117–141.
[8] A.G.H. Dietz, in: R.W. Hamilton (Ed.), Diathermanous Materials and Properties of Surfaces in Space Heating with Solar Energy, MIT Press, Cambridge MA, 1954, pp. 25–43.
[9] J.A. Duffie, W.A. Beckman, Solar Engineering of Thermal Processes, Wiley, New York, 1980.
[10] I. Kirk, D.F. Othmer (Eds.), Encyclopedia of Chemical Technology, Wiley, New York, 1982.
[11] G.R. Guinn, B.R. Hall, Solar production of industrial process hot water using shallow solar ponds, in: Proc. Solar Industrial Process Heat Symp, 1977, pp. 161–169.
[12] F.P. Incopera, D.P. DeWitt, Fundamentals of Heat and Mass Transfer, Wiley, New York, 1985.
[13] W.M. Keys, Convective Heat and Mass Transfer, McGraw-Hill, New York, 1966.
[14] P. Madsen, K. Goss, Report on nonmetallic solar collectors, Solar Age 6 (1) (1981) 28–32.
[15] Th. Baumaister, E. Avallone (Eds.), Mark's Standard Handbook for Mechanical Engineers, McGraw Hill, New York, 1978.
[16] Materials Reference Issue, Mashine Design, 51 (6) March 15, 1979.
[17] F.C. O'Brien-Bernini, J.G. McGowan, Performance modelling of non-metallic flat plate solar collectors, Solar Energy 33 (3/4) (1984) 305–319.
[18] W.J. Platzer, Total heat transport data for plastic honeycomb-type structures, Type Structures, Solar Energy 49 (5) (1992) 351–358.
[19] P.T. Tsilingiris, Third Party Financing for Active Solar Systems in Greece, in: Presented at the 1st European Solar Industry Federation (E.S.I.F.) meeting, Marseilles, France, Centre for Renewable Energy Sources, Athens, 1993.
[20] P.T. Tsilingiris, Design, analysis and performance of low-cost plastic film large solar water heating systems, Solar Energy 60 (5) (1997) 245–256.
[21] VDI Warmeatlas, Berechnungsblatter fur den Warmeubergang, Sechste Erweiterte Auflage, VDI Verlag GmbH, Dusseldorf, 1991.
[22] D. Waksman, A. Dawson, The influence of environmental exposure on solar collectors and their materials, Proc. of the AS/ISES Conf 3.1 (1980) 415–419.
[23] H.R. Wilson, Transmission switching using micro-encapsulated liquid crystal films, Solar Energy 49 (5) (1992) 435–445.